PHYSICAL REVIEW C **80**, 045207 (2009)

Structure of the $X(1835)$ baryonium

J.-P. Dedonder* and B. Loiseau†
Laboratoire de Physique Nucléaire et de Hautes Énergies, Groupe Théorie, IN2P3-CNRS, Universités Pierre & Marie Curie et Paris Diderot, 4 Place Jussieu, F-75252 Paris, Cedex, France

B. El-Bennich‡
Physics Division, Argonne National Laboratory, Argonne, Illinois 60439, USA

S. Wycech§
Sołtan Institute for Nuclear Studies, Warsaw, Poland
(Received 14 April 2009; published 16 October 2009)

The measurement by the BES Collaboration of $J/\psi \to \gamma p\bar{p}$ decays indicates an enhancement at the $p\bar{p}$ threshold. In another experiment, BES finds a peak in the invariant mass of π mesons produced in the possibly related decay $J/\psi \to \gamma\pi^+\pi^-\eta'$. Using a semiphenomenological potential model that describes all the $N\bar{N}$ scattering data, we show that the explanation of both effects may be given by a broad quasibound state in the spin and isospin singlet S wave. The structure of the observed peak is due to an interference of this quasibound state with a background amplitude and depends on the annihilation mechanism.

DOI: 10.1103/PhysRevC.80.045207 PACS number(s): 14.40.Gx, 12.39.Pn, 13.75.Cs

I. INTRODUCTION

The search for exotic states in the $N\bar{N}$ systems has been pursued for a few decades, but significant results have only been obtained recently. An indication of such states below the $N\bar{N}$ threshold may be given by the scattering lengths for a given spin and isospin state. However, in scattering experiments, it is difficult to assess a clear separation of quantum states. Measurements of the X-ray transitions in the antiproton hydrogen atom can select some partial waves if the fine structure of atomic levels is resolved. Such resolution has been achieved for the $1S$ states [1] and partly for the $2P$ states [2]. One can also use formation experiment methods to reach specific states. In this way, an enhancement close to the $p\bar{p}$ threshold has been observed by the BES Collaboration [3] in the radiative decay

$$J/\psi \to \gamma p\bar{p}. \tag{1}$$

On the other hand, a clear threshold suppression is seen in the decay channel $J/\psi \to \pi^0 p\bar{p}$. To understand better the nature of these $p\bar{p}$ states, one has to look directly into the subthreshold energy region. This may be achieved in the antiproton-deuteron or the antiproton-helium reactions at zero or low energies. Such atomic experiments have been performed, although the fine structure resolution has not been reached so far [4,5]. Another way to look below the threshold is by the detection of $N\bar{N}$ decay products. Recently the reaction

$$J/\psi \to \gamma\pi^+\pi^-\eta' \tag{2}$$

was studied by the BES Collaboration [6]. This reaction is attributed [6] to an intermediate $p\bar{p}$ configuration in the $J^{PC}(p\bar{p}) = 0^{-+}$ state which corresponds to spin singlet S-wave state. A peak in the invariant meson mass is observed and interpreted as a new baryon state, named $X(1835)$. The interpretation of the peak as a new $X(1835)$ has been questioned by the Jülich group [7]. The latter view is supported by our calculations, but we suggest the origin of the BES finding to differ from the possibilities presented in Ref. [7]. It is argued here that the peak is due to an interference of a quasibound, isospin 0, $N\bar{N}$ state with a background amplitude. The same quasibound state was found in Ref. [8] to be responsible for the threshold enhancement in reaction (1).

The purpose of the present work is to discuss the physics of $N\bar{N}$ states produced in these J/ψ decays and relate it to atomic experiments. In reaction (1), only three $p\bar{p}$ final states are possible, as a consequence of the J^{PC} conservation. These differ by the internal angular momenta and spins. Close to the $p\bar{p}$ threshold, a distinctly different behavior of scattering amplitudes is expected in different states. A further selection of states is possible, but one has to rely on the analyses of the elastic and inelastic $N\bar{N}$ scattering experiments. This has been studied in Ref. [8] within the Paris potential model [9–12], which is also used in the present work.

The final $p\bar{p}$ states allowed by P and C conservation in the $\gamma p\bar{p}$ channel are specified in Table I. These are denoted as $^{2S+1}L_J$ or $^{2I+1,2S+1}L_J$, where S, L, and J are the spin, angular momentum, and total momentum of the pair, respectively, while I denotes the isospin. A unified picture and a better specification in the radiative decays is achieved, semiquantitatively, with an effective three-gluon exchange model [8]. This description indicates the final $\gamma p\bar{p}$ state to be dominated by the $p\bar{p}$ $^{11}S_0$ partial wave. In this wave, the Paris potential generates a 52 MeV broad quasibound state at 4.8 MeV below threshold. This state is named $N\bar{N}_S(1870)$. A similar conclusion has been reached by the Jülich group, although the Bonn-Jülich potential does not generate a bound state in the $p\bar{p}$ $^{11}S_0$ partial wave [7].

*dedonder@univ-paris-diderot.fr
†loiseau@lpnhe.in2p3.fr
‡bennich@anl.gov
§wycech@fuw.edu.pl

TABLE I. States of the low-energy $p\bar{p}$ pairs allowed in the $J/\psi \to \gamma p\bar{p}$ decays. The first column gives the decay modes to the specified internal states of the $p\bar{p}$ pair. The J^{PC} for the photon is 1^{--}. The second column gives the J^{PC} for the internal $p\bar{p}$ system, the last column gives the relative angular momentum of the photon vs the pair. $J^{PC} = 1^{--}$ for J/ψ.

Decay mode	$J^{PC}(p\bar{p})$	Relative l
$\gamma p\bar{p}(^1S_0)$	0^{-+}	1
$\gamma p\bar{p}(^3P_0)$	0^{++}	0
$\gamma p\bar{p}(^3P_1)$	1^{++}	0

Under the assumption that the π^+, π^-, and η' are produced in relative S waves, reaction (2), if attributed to an intermediate $p\bar{p}$ as suggested by the BES group, is even more restrictive than reaction (1). It allows only one intermediate state, the $p\bar{p}\,^1S_0$, which coincides with the previous findings. The presence of an intermediate $p\bar{p}$ state in reaction (2) is possible but not granted. We show below that a more consistent interpretation is obtained with the dominance of the $N\bar{N}(1870)$ state, which is a mixture of $p\bar{p}$ and $n\bar{n}$ pairs.

The content of this work is as follows. Section II contains a description of the final state $p\bar{p}$ interaction and is included here for completeness. The subthreshold $N\bar{N}$ scattering amplitude, needed to describe reaction (2), is defined in Sec. III. Section IV gives the equation to be solved to calculate the amplitude of the meson formation through the intermediate $N\bar{N}$ interaction. The results are presented and discussed in Sec. V together with some concluding remarks.

II. FINAL STATE INTERACTIONS

For any multichannel system at low energies, described by an S-wave K matrix, the transition amplitude from an initial channel i to a final channel f may be described by

$$T_{if} = \frac{A_{if}}{1 + iq_f A_{ff}}, \tag{3}$$

where A_{if} is a transition length, A_{ff} is the scattering length in the channel f, and q_f is the momentum in this channel [13]. In the following, channel f is understood to be the $p\bar{p}$ channel. Within the same formalism, the scattering amplitude in channel f reads

$$T_{ff} = \frac{A_{ff}}{1 + iq_f A_{ff}}. \tag{4}$$

For S waves at low energies, A_{if}, A_{ff} are functions of q_f^2 and the main energy dependence of the amplitudes comes from the denominators in Eqs. (3) and (4). With large values of Re $A_{ff} > 0$, one may expect a bound (quasibound) state. For large Re $A_{ff} < 0$, a virtual state is likely, but one cannot determine these properties with absolute certainty unless a method to extrapolate below the threshold exists. This is particularly true in the $p\bar{p}$ case, where the absorptive part Im A_{ff} is large

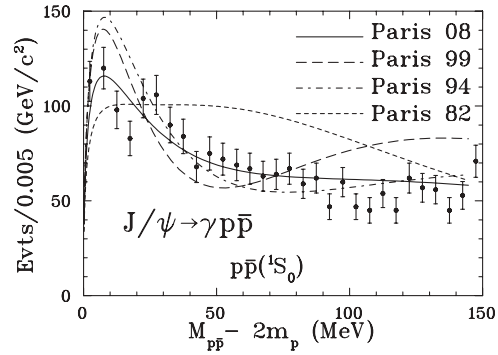

FIG. 1. Final state factor $q_f|T_{if}|^2$ for the J/ψ decays into γ and $p\bar{p}$. The latest version of the Paris model generates a quasibound state of $\Gamma = 52$ MeV and 4.8 MeV binding energy and is the most consistent with the data.

because of the presence of many open annihilation channels. Since the final photon interactions are believed to be negligible, the energy dependence observed in the $J/\Psi \to \gamma p\bar{p}$ decay rate reflects the energy dependence in $q_f|T_{if}|^2$.

Practical calculations also indicate an energy dependence in A_{ff} and the Watson approximation, i.e., the constant A_{if} is not applicable in a broader energy range. One needs to use Eq. (3) and a weakly energy-dependent formation amplitude $A_{if} \sim 1/(1 + q_f^2 r_i^2)$ as explained in Ref. [8], where a best fit value $r_i = 0.55$ fm was found. Figure 1 displays sizable model dependence of $q_f|T_{if}|^2$ for the $^1S_0$ calculated for four versions of the Paris potential model [9–12]. These versions followed the increasing data basis which, for the most recent case, includes antineutron scattering and antiprotonic hydrogen data. The threshold enhancement is attributed to a strong attraction in this partial wave. It does not prove the existence of a quasibound state, but such a state is indeed generated by the model in the $^{11}S_0$ wave [9]. There are additional arguments to support this result which follow from light $\bar{p}$ atoms. The absorptive amplitudes can be extracted from the atomic level widths. With the data from Refs. [4,5] such an extraction was described in Refs. [14] and [15]. The data allow one to obtain only an isospin-spin average, but as indicated in Fig. 2, the existence of a quasibound state is consistent with the atomic data. The increase of subthreshold absorption is also supported by the atomic level widths in heavy $\bar{p}$ atoms [15]. In addition to the broad S-wave state, the Paris potentials generate a narrow $^{33}P_1$ quasibound state, which arises in Paris 08 and Paris 99 potentials. It gains some support from widths in the antiprotonic deuterium as indicated in Fig. 2.

The procedure outlined above is based on a simple form of the low-energy final state wave function $\Psi_{p\bar{p}}$. At large distances and for small $q_f r$, it becomes

$$\Psi(r)_{p\bar{p}} \sim 1 - \frac{T_{ff}\ \exp(iq_f r)}{r} \approx [1 - A_{ff}/r]\frac{1}{1 + iq_f A_{ff}}. \tag{5}$$

The right side of this relation expands the wave up to q_f^2 terms. At shorter distance, the wave function is no more directly related to the scattering matrix and depends on details of the

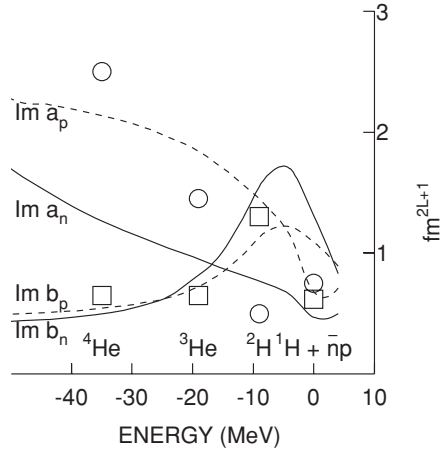

FIG. 2. Absorptive parts of spin-isospin averaged $N\bar{p}$ scattering amplitudes extracted from the atomic level widths in H, ^{2}H, ^{3}He, and ^{4}He$\bar{p}$ [14]. Squares: S waves; circles: P waves. The bottom scale indicates the energy below threshold. The curves, calculated with the Paris 2008 potential, give the amplitudes separately: $a_{n(p)}$ denote the $n\bar{p}$ or $p\bar{p}S$-wave amplitudes, respectively, and $b_{n(p)}$ the corresponding P-wave amplitudes. The strong increase of absorption in the $\bar{p}p$ S wave is attributed mainly to the $^{11}S_0$ state.

interaction in channel f. Integrated over an unknown transition potential V_{if} it generates the formation amplitude A_{if} in the transition amplitude T_{if}. Equation (3) was used with the Paris [8] and Jülich [16] potentials. These potentials also generated the A_{ff}. Formulas (3) or (5) are useful above the threshold but cannot be simply extrapolated to the subthreshold region. The difficulty is related to the momentum $q_f = \sqrt{2\mu_{N\bar{N}} E_{N\bar{N}}}$ where $\mu_{N\bar{N}}$ is the reduced mass. Above the threshold, $E_{N\bar{N}}$ is the kinetic energy in the c.m. system; below the threshold, $E_{N\bar{N}}$ is negative and q_f becomes imaginary. The outgoing wave $\exp(iq_f r)/r$ becomes $\exp(-|q_f|r)/r$. It damps strongly the interaction term in Eq. (5) and a more precise description is necessary. We now turn to this point.

III. OFF-SHELL $N\bar{N}$ INTERACTIONS

For further calculations, one needs the off-shell extension of the scattering amplitude in the energy as well as in the momentum variables. The most general extension for S waves is given by

$$f(k, E, k') = \frac{\mu_{N\bar{N}}}{2\pi} \int \psi_o(r, k) V_{N\bar{N}}(r, E) \Psi^+(r, E, k') r^2 \, dr, \tag{6}$$

where $\Psi^+(r, E, k')$ is the full outgoing wave calculated with the regular free wave $\psi_o(r, k') = \sin(rk')/(rk')$. In this equation, the momentum k' is not related to the energy E. The Fourier-Bessel double transform of $f(k, E, k')$ would generate a nonlocal $\widetilde{f}(r, E, r')$ matrix in the coordinate representation. Therefore, involved calculations do not seem necessary, because the experimental data are rather crude. We resort to a simpler procedure, standard in nuclear physics (for an application in the antiproton physics see Ref. [17]). The subthreshold scattering amplitudes are calculated in terms of

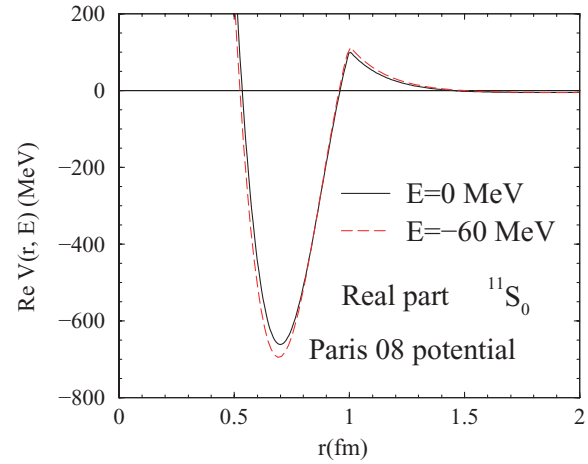

FIG. 3. (Color online) Real Re $V(r, E)$ potential for $N\bar{N}$ interactions in the $^{11}S_0$ state.

the T matrix defined in the coordinate representation by

$$\widetilde{T}(r, E) = \frac{\mu_{N\bar{N}}}{2\pi} V_{N\bar{N}}(r, E) \frac{\Psi^+(r, E, k'(E))}{\psi_o(r, k'(E))}, \tag{7}$$

with $k'(E) = \sqrt{2\mu_{N\bar{N}} E}$. The $\widetilde{T}(r, E)$ is a local equivalent of the nonlocal T matrix in the sense that matrix elements in the S waves fulfill the relation $f(k, E, k'(E)) = \int dr \; r^2 \; \psi_o(r, k) \widetilde{T}(r, E) \psi_o(r, k'(E))$ valid in a narrow subthreshold region where the last integral is convergent. The $V_{N\bar{N}}(r, E)$ is the recent Paris interaction potential [9] which is used in the Schrödinger equation to calculate $\Psi^+(r, E, k'(E))$. The potentials used are plotted in Figs. 3 and 4, and the resulting scattering amplitude is given in Fig. 5.

To describe the intermediate $N\bar{N}$ state, we need also the Fourier transform of $T(r, E)$

$$T(\kappa, E) = \int d\mathbf{r} \, \widetilde{T}(r, E) \frac{\sin(\kappa r)}{\kappa r}. \tag{8}$$

In the next step, Eq. (8) is used at negative energies $E = E_{N\bar{N}}$. For positive energies, this equation is not practical because of the zeros in the denominator that occur in $\widetilde{T}(r, E)$ [see

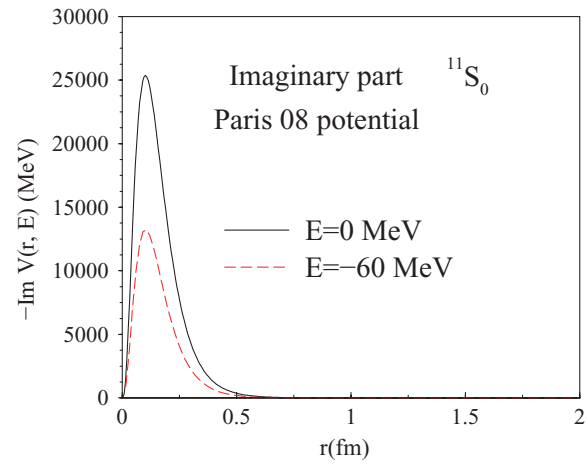

FIG. 4. (Color online) Absorptive $-\mathrm{Im}V(r, E)$ potential for $N\bar{N}$ interactions in the $^{11}S_0$ state.

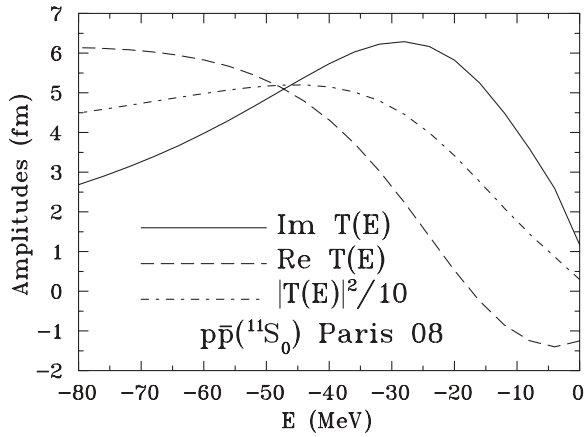

FIG. 5. Real Re $T(E)$ and imaginary Im $T(E)$ parts for $N\bar{N}$ scattering amplitude in the $^{11}S_0$ state.

Eq. (7)] at multiplicities of $k' = \pi/r$. One could nevertheless use it for $k' < \pi/r_{\max}$, where $r_{\max}$ is the distance at which the potential is cut off. One has to set $r_{\max} \simeq 2$ fm if one wants to extend the calculations up to energies of ≈ 20 MeV above the $N\bar{N}$ threshold. The normalization of $\widetilde{T}(r, E)$ by $\psi_o(r, k'(E))$ in Eq. (7) ensures the convergence of the integral [Eq. (8)] below threshold. To see the predictions of our model above threshold, we shall replace in Eq. (7) $\psi_o(r, k'(E))$ by unity for $E \geqslant 0$.

The relevant on-shell S-wave scattering amplitudes given by

$$T(E) = \int d\mathbf{r}\, \widetilde{T}(r, E) \tag{9}$$

are normalized to the corresponding scattering lengths at the threshold. The results for $T(E)$ are plotted in Fig. 5. One can notice a resonant behavior of the imaginary part. Roughly, the structure of this amplitude is dominated by the weakly bound state $N\bar{N}_S(1870)$ in this wave. However, the location of the bound state given as a pole in the complex energy plane (Re $E = 1871.7$ MeV, $\Gamma = 52$ MeV) corresponds neither to the maximum in the Im $T(E)$ which occurs at $E \approx 1840$ MeV nor to the maximum of the $\pi^+\pi^-\eta'$ invariant-mass distribution that occurs at 1835 MeV. The interpretation of the $X(1835)$ turns out to be more involved.

The potentials that generate this state are plotted in Figs. 3 and 4. The real potential (Fig. 3) contains a very weak attractive tail, a repulsive barrier, a strong energy-dependent attraction in the 0.5–1.0 fm range, and a repulsive core [11]. These features, modified by the energy-dependent annihilation potential (Fig. 4) and the proximity of the threshold, generate a rather untypical $N\bar{N}$ scattering matrix in the subthreshold energy region. The width of the $^{11}S_0$ bound state indicates some energy dependence. Moreover, the bound-state form factor displays strong enhancement in the subthreshold region, which is a typical phenomenon of the subthreshold extrapolations. Altogether, a strong enhancement of Im T is generated in the region well below the actual binding energy. As discussed above, this effect finds support in the widths of the $\bar{p}$-atom levels indicated in Fig. 2.

IV. THE INTERMEDIATE $p\bar{p}$ STATES

We assume that the photon in reaction (2) is emitted before the annihilation into mesons has taken place, as it happens in reaction (1). A specific model for that process was suggested in Ref. [8], but it will not be needed here. We assume, however, that the formation of the $N\bar{N}$ pair is described by a source function $F_{i,f}$ and the annihilation by another function $F_{f,\text{mes}}$. In this way, the effect of the intermediate $N\bar{N}$ interactions can be described by an amplitude for the meson formation

$$T_{i,\text{mes}} = \int d\mathbf{p}\, d\mathbf{p}' F_{i,f}(p)\, G(\mathbf{p}, \mathbf{p}', E_{N\bar{N}}) F_{f,\text{mes}}(p', Q), \tag{10}$$

where $G(\mathbf{p}, \mathbf{p}', E_{N\bar{N}})$ is the full Green's function for the intermediate $N\bar{N}$ system. The form assumed for the annihilation amplitude is

$$F_{f,\text{mes}}(p', Q) = \left\langle \exp\left(-(\mathbf{Q} - \mathbf{p}')^2 r_f^2\right)\right\rangle, \tag{11}$$

where the angular average over $\mathbf{Q}$ is indicated by the brackets. This choice is motivated by simple model considerations and the simplest possible assumption that the two π mesons in reaction (2) are correlated to the $f_0(600)$ (also named σ meson). The mass of the latter is assumed to be 500 MeV in our calculations. The relative momentum[1] of the final η' and σ mesons is denoted by $\mathbf{Q}$, while the Gaussian profile comes from quark rearrangement models of annihilation which operate Gaussian wave functions.

The Green's function in Eq. (10) may be expressed in terms of the free Green's function G_o and the $N\bar{N}$ scattering amplitude T as

$$G = G_o + G_o T G_o. \tag{12}$$

Now, with the scattering amplitude defined by Eq. (7) and Eq. (8), one obtains

$$T_{i,\text{mes}} = \int d\mathbf{p} d\mathbf{p}' F_{i,f}(p) G_o(p, E_{N\bar{N}})[\delta(\mathbf{p} - \mathbf{p}') + T(|\mathbf{p} - \mathbf{p}'|, E_{N\bar{N}}) G_o(p', E_{N\bar{N}})] F_{f,\text{mes}}(p'). \tag{13}$$

The first term in Eq. (13) corresponds to a background amplitude with a noninteracting $N\bar{N}$ pair. The second one describes intermediate state interactions. Green's function is $G_o(p, E) = 4\pi/[(2\pi)^3(q_f^2 - p^2)]$, and the normalization is chosen such that T in Eq. (13) has dimension of length. Let us notice that below the $N\bar{N}$ threshold, both q_f^2 and G_o are negative. Below the quasibound state, T is attractive (negative) and the interference in Eq. (13) becomes constructive. This effect extends the peak structure to lower energies. We assume the formation amplitude to be described by

$$F_{i,f}(p) = \frac{1}{1 + p^2 r_i^2}, \tag{14}$$

with the range parameter $r_i = 0.55$ fm determined before from the final interactions above the threshold [8]. The

[1]Denoting by M_N, m_σ, and $m_{\eta'}$ the masses of the nucleon, σ and η' mesons, respectively, one has $\sqrt{m_\sigma^2 + \mathbf{Q}^2} + \sqrt{m_{\eta'}^2 + \mathbf{Q}^2} = 2M_N - |E_{N\bar{N}}|$.

normalization is arbitrary. The angular integrations in Eq. (13) generate an amplitude that depends only on $|\mathbf{Q}|$; that is due to the momentum dependence of the half-off shell T matrix and to the absence of any preferred direction in the initial $N\bar{N}$ state.

A semifree parameter r_f is related to the radius parameter in the quark models for the nucleon and mesons. The range of allowed r_f values is limited. The upper limit $r_f \approx 0.55$ fm is obtained assuming the rms radii of the quark densities to be equal to the electromagnetic radii (0.8 fm for baryons and 0.6 fm for mesons). A lower limit $r_f \approx 0.25$ fm is obtained with the radii used in NN interaction models based on quark approaches [18] and quark rearrangement models of $N\bar{N}$ annihilation [19]. These rely on rms radii in the range 0.5–0.6 fm for baryons and 0.4–0.6 fm for mesons.

The last factor needed in this calculation involves the four-body phase space for $J/\psi \to \gamma\pi^+\pi^-\eta'$. We follow Ref. [13] to find

$$dL_4(M_J^2; P_\gamma, P_{\pi^+}, P_{\pi^-}, P_{\eta'}) = \frac{(M_J^2 - S_M)}{(2\pi)^2 4M_J^2} dL_3(S_M; P_{\pi^+}, P_{\pi^-}, P_{\eta'}) dS_M, \quad (15)$$

where M_J is the mass of J/ψ and dL_3 is the invariant phase space for the three-meson system of invariant mass squared S_M. The dL_3 may be found in Ref. [20], and it generates only a weak energy dependence. The full phase space is used, but one finds a simple approximation $dL_4 \sim \varepsilon/(m_{\eta'} + 2m_\pi + \varepsilon)^2$ with $\varepsilon = \sqrt{S_M} - m_{\eta'} - 2m_\pi$ to work well in the whole region of interest.

All together, the spectral function representing the $X(1835)$ is given by

$$X_S = |T_{i,\mathrm{mes}}|^2 dL_4/dS_M. \quad (16)$$

V. RESULTS AND CONCLUDING REMARKS

The best description of the BES data is obtained with $r_f \approx$ 0.4–0.5 fm, and the shape of $X(1835)$ calculated in this way is given in Fig. 6. The intermediate state is the isospin 0 state. The data are reproduced fairly well despite the fact that the bound state itself occurs at 1871.7 MeV, i.e., 4.8 MeV below the threshold. This shape is determined by the interference effect of the two terms in Eq. (13) describing the decay process. Within the Paris potential model and within a broad range of semifree r_i, r_f parameters, one finds no peak structure with the intermediate $p\bar{p}$ state. This result is consistent with the observation that isospin 1 for the final mesons is not allowed and the decay $N\bar{N}(T = 1) \to \pi^+\pi^-\eta'$ is not permitted by the isospin conservation [19].

Other contributions, possible improvements. Above the $N\bar{N}$ threshold, our estimation of X_S from our model Eq. (13) using Eq. (8) with Eq. (7), where $\psi_o(r, k'(E))$ is replaced by unity [see our discussion in Sec. II just below Eq. (8)] generate a minimum (see Fig. 6) that is deeper than the minimum indicated by the data. Below we indicate several possible explanations.

(i) The J^{PC} conservation allows the $N\bar{N}$ pair in the $^{11}S_0$ state to decay into the $f_0(600)\eta'$ pair in a relative S wave. This case has been discussed so far. In addition, with the baryons in $^{13}P_1$ states another decay mode to the $f_0(600)\eta'$ pair is possible. It requires the two final mesons to be in the relative P-wave state. In the recent Paris 08 [9] as well as in the former Paris 99 potential [10], a close to threshold resonance is generated in the related $^{13}P_1$ state. With the energy $E_P = 1872$ MeV and width $\Gamma_P = 20$ MeV, it may contribute a spike to the spectral distribution in Fig. 6. Since two different partial waves are involved in the final states, such a decay produces no interference with the main mode and could contribute a term

$$X_P = \left| \frac{C_P Q}{E_{N\bar{N}} - E_p + i\Gamma_p/2} \right|^2 dL_4/dS_M \quad (17)$$

to be added to the main expression for X_S given in Eq. (16). The X_P possibility is a speculative one, and the relative strength C_P would be very hard to predict. Also, with the recent update of the Paris potential, the position of the P-wave resonance is not generated at the "proper" position.

(ii) In a more complete study, outside the scope of the present work, one could extend our S-wave equations [Eqs. (7), (8), and (13)] to the P-wave case. Here we illustrate in Fig. 7 the possible effect of an effective P wave represented by a resonant term given by Eq. (17). It can be seen that such an effective resonance with $E_p = 1900$ MeV and $\Gamma_p = 200$ MeV can fill up the above threshold dip of X_S.

(iii) The off-shell extension in terms of Eq. (7) cannot be fully trusted, and the procedure of Eq. (6) should be used.

(iv) The final state factor given by Eq. (11) is perhaps too simple to be used above the $N\bar{N}$ threshold. In some decay models, an energy-dependent phase factor F_{mes} is expected [19]. This would have a very limited effect below the threshold, since the loop integrals over G_o generate real functions. However, above the threshold,

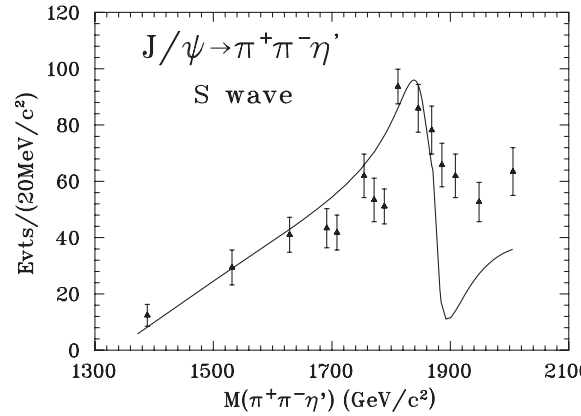

FIG. 6. Spectral function X_S representing the $X(1835)$ shape. Here the range parameter of the annihilation amplitude [Eq. (11)] is $r_f = 0.45$ fm. This S-wave contribution has been normalized to reproduce the data close to the $X(1835)$ peak. The experimental points are from Ref. [6]. Above the $N\bar{N}$ threshold, the calculation is performed replacing $\psi_o(r, k'(E))$ by unity in Eq. (7).

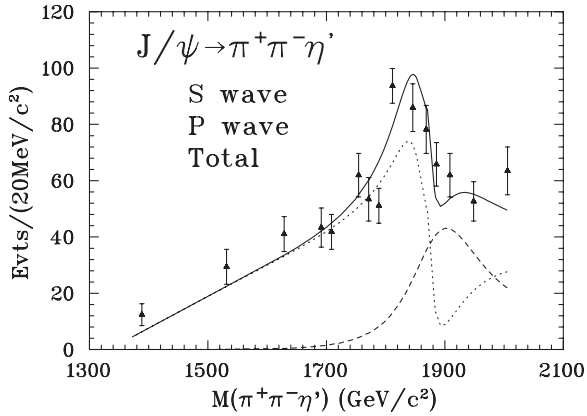

FIG. 7. Spectral functions X_S (calculated as for Fig. 6) and X_P [Eq. (17) with $E_p = 1900$ MeV and $\Gamma_p = 200$ MeV] and their sum representing the $X(1835)$ shape. Here the S- and P-wave contributions have been normalized to reproduce the data [6].

the loop integral becomes complex, and the interference pattern seen in Fig. 6 might be changed.

These effects go beyond the technique used in this paper.

(v) To confirm experimentally a direct link between the $p\bar{p}$ system and the $X(1835)$, authors of Ref. [7] have suggested a search at the future GSI Facility for Antiproton and Ion Research (FAIR) project using the proton antiproton detector array (PANDA) in reactions such as $\bar{p}p \to \pi^+\pi^- X$ and $X \to \pi^+\pi^-\eta'$. Another possible reaction would be $\bar{p}p \to \gamma X(1835)$. It could be performed with the Polarized Antiproton Experiment (PAX) apparatus [21] with ~ 50 MeV polarized antiprotons on polarized protons at the CERN antiproton decelerator (AD) ring. The shape of the $X(1835)$ could be tested by the photon energy distribution. Of special value would be the comparison of two measurements obtained with the parallel and antiparallel initial spin configurations. That could give information on the mechanism of the $X(1835)$ formation. In particular, it would check the simple model presented in Ref. [8], where the initial state (in the J/Ψ case, the intermediate) of the $p\bar{p}$ system is the spin triplet, which, after the emission of a magnetic photon, turns into the final spin singlet.

In summary. It is shown that the $X(1835)$ structure can be generated by a conventional $N\bar{N}$ potential model. Such a structure stems from a broad and weakly bound state, the $N\bar{N}_S(1870)$ that exists in the $^{11}S_0$ wave. The existence of a quasibound S-wave state receives an additional confirmation from the level widths of antiprotonic atoms.

ACKNOWLEDGMENTS

We thank M. Lacombe for useful discussions. This research was performed in the framework of the IN2P3-Polish Laboratory Convention (Collaboration No. 05-115). S.W. was supported by the EC 6-Th Program MRTN-CT-206-03502 (FLAVIA network). This work was also supported in part by the US Department of Energy, Office of Nuclear Physics, Contract No. DE-AC02-06CH11357.

[1] M. Augsburger *et al.*, Phys. Lett. **B461**, 417 (1999).
[2] M. Augsburger *et al.*, Nucl. Phys. **A658**, 149 (1999).
[3] J. Z. Bai *et al.* (BES Collaboration), Phys. Rev. Lett. **91**, 022001 (2003).
[4] D. Gotta *et al.*, Nucl. Phys. **A660**, 283 (1999).
[5] M. Schneider *et al.*, Z. Phys. A **338**, 217 (1991).
[6] M. Ablikim *et al.* (BES Collaboration), Phys. Rev. Lett. **95**, 262001 (2005).
[7] J. Haidenbauer, Ulf-G. Meißner, and A. Sibirtsev, Phys. Rev. D **74**, 017501 (2006).
[8] B. Loiseau and S. Wycech, Phys. Rev. C **72**, 011001(R) (2005).
[9] B. El-Bennich, M. Lacombe, B. Loiseau, and S. Wycech, Phys. Rev. C **79**, 054001 (2009).
[10] B. El-Bennich, M. Lacombe, B. Loiseau, and R. Vinh Mau, Phys. Rev. C **59**, 2313 (1999).
[11] M. Pignone, M. Lacombe, B. Loiseau, and R. Vinh Mau, Phys. Rev. C **50**, 2710 (1994).
[12] J. Côté, M. Lacombe, B. Loiseau, B. Moussalam, and R. Vinh Mau, Phys. Rev. Lett. **48**, 1319 (1982).
[13] H. Pilkuhn, *The Interaction of Hadrons* (North-Holland, Amsterdam, 1967), p. 167.
[14] S. Wycech and B. Loiseau, AIP Conf. Proc. **796**, 131 (2005).
[15] S. Wycech, F. J. Hartmann, J. Jastrzebski, B. Klos, A. Trzcinska, and T. von Egidy, Phys. Rev. C **76**, 034316 (2007).
[16] A. Sibirtsev, J. Haidenbauer, S. Krewald, Ulf-G. Meißner, and A. W. Thomas, Phys. Rev. D **71**, 054010 (2005).
[17] A. M. Green and S. Wycech, Nucl. Phys. **A377**, 441 (1982).
[18] M. Lacombe, B. Loiseau, R. Vinh Mau, P. Demetriou, J. P. B. C. de Melo, and C. Semay, Phys. Rev. C **65**, 034004 (2002).
[19] A. M. Green and J. A. Niskanen, Nucl. Phys. **A412**, 448 (1984).
[20] G. Källén, *Elementary Particle Physics* (Addison-Wesley, Reading, MA, 1964), p. 433.
[21] P. Lenisa and F. Rathmann (PAX Collaboration), arXiv:0904.2325 [nucl-ex]; CERN-SPSC-2009-012/SPSC-P-337-2009 (unpublished).